Optics Letters

Optically injected InAs/GaAs quantum dot laser for tunable photonic microwave generation

Cheng Wang,[1,2] Ravi Raghunathan,[1] Kevin Schires,[1] Sze-Chun Chan,[2,3] Luke F. Lester,[4] and Frédéric Grillot[1,5,*]

[1]CNRS LTCI, Télécom ParisTech, Université Paris Saclay, 46 rue Barrault, F-75634 Paris Cedex 13, France
[2]Department of Electronic Engineering, City University of Hong Kong, Hong Kong, China
[3]State Key Laboratory of Millimeter Waves, City University of Hong Kong, Hong Kong, China
[4]Department of Electrical and Computer Engineering, Virginia Tech, Blacksburg, Virginia 24061-0111, USA
[5]Center for High Technology Materials, University of New Mexico, 1313 Goddard SE, Albuquerque, New Mexico 87106-4343, USA
*Corresponding author: grillot@telecom-paristech.fr

Received 24 December 2015; revised 29 January 2016; accepted 4 February 2016; posted 4 February 2016 (Doc. ID 256403); published 8 March 2016

We present an experimental investigation on the period-one dynamics of an optically injected InAs/GaAs quantum dot laser as a photonic microwave source. It is shown that the microwave frequency of the quantum dot laser's period-one oscillation is continuously tunable through the adjustment of the frequency detuning. The microwave power is enhanced by increasing the injection strength providing that the operation is away from the Hopf bifurcation, whereas the second-harmonic distortion of the electrical signal is well reduced by increasing the detuning frequency. Both strong optical injection and high detuning frequency are favorable for obtaining a single sideband optical signal. In addition, particular period-one oscillation points of low sensitivity to the frequency detuning are found close to the Hopf bifurcation line.

OCIS codes: (250.5960) Semiconductor lasers; (250.5590) Quantum-well, -wire and -dot devices; (140.3520) Lasers, injection-locked; (350.4010) Microwaves.

http://dx.doi.org/10.1364/OL.41.001153

Semiconductor lasers can generate a large variety of nonlinear dynamics when subject to optical injection or optical feedback, including stability and bistability, periodic and quasiperiodic oscillations, as well as chaos [1]. Among these rich dynamics, chaos has been intensively explored for applications in secured communication and random bit generations [2–5]. On the other hand, exploitation of the period-one (P1) oscillation is of importance for the development of radio-over-fiber communication systems, photonic microwave signal processing, and beamforming [6–13]. The P1 oscillation is invoked when the optical injection is operated above the Hopf bifurcation in the injection-locking diagram formed by the injection ratio and the detuning frequency [14–16]. The injection ratio is usually defined as the ratio between the optical power injected from the master laser to the slave laser and the free-running emission power of the slave laser. The detuning frequency refers to the frequency offset of the master laser with respect to the slave laser when free-running. In contrast to many other photonic microwave-generation techniques [16–18], the P1 oscillation offers the following merits:

(i) It is a low-cost all-optical configuration without using high-speed electronic components [6,16].
(ii) The oscillation frequency is widely tunable either by adjusting the injection ratio or by the detuning frequency. The frequency ranges from the laser's relaxation resonance frequency up to the millimeter-wave band [12].
(iii) The optical signal has a nearly single sideband (SSB) spectrum, which is beneficial for reducing the chromatic dispersion-induced power penalty during data transmission in optical fibers [7].
(iv) The oscillation can yield an intensity modulation depth of up to 100% [6,11].

In contrast to quantum well (Qwell) lasers, semiconductor emitters based on the quantum dot (Qdot) structure are known to exhibit superior characteristics like a lower threshold current density [19,20] and a better temperature stability [21], owing to the ultimate 3D quantum confinement of carriers [22]. Besides, prior arts have unveiled the highly damped feature of Qdot lasers [23] associated with the reduced linewidth enhancement factor (α-factor), which leads to less occurrences of complicated nonlinear dynamical behaviors [1]. Consequently, Qdot lasers show an increased stability and produce less complicated trajectories and smaller regions of chaotic dynamics when subject to optical injection or optical feedback [24,25]. In addition, Qdot lasers were observed to produce phase-locked bistability between two steady states of different optical intensities, which is typically a feature of class-A lasers [26,27]. There have been only a few reports on the

investigation of a Qdot laser's P1 dynamics. References [28,29] theoretically calculated the P1 oscillation regions of optically injected Qdot lasers based on the analysis of bifurcation scenarios. Pochet *et al.* studied the bifurcation diagram [30] and analytically analyzed the P1 oscillation frequency of an optically injected quantum dash (Qdash) laser with a maximum value of 8 GHz [31]. In addition, Hurtado *et al.* reported an interesting experimental demonstration on the variation of the P1 oscillation frequency up to 40 GHz, as well as the associated fundamental microwave power for positively detuned injection [32]. Very recently, Chen *et al.* reported that the optical spectrum of a Qdot laser's P1 oscillation exhibited a better SSB performance than that in a Qwell laser [33]. In this work, we aimed to systematically investigate the P1 dynamics of an optically injected InAs/GaAs Qdot laser. The P1 dynamics are examined over a range of injection conditions that include both positive and negative detuning frequencies. The fundamental P1 microwave is investigated along with the oscillation frequency. Then, the optical sideband rejection ratio is studied to quantify the SSB operation. The second harmonic of the microwave is examined as well.

The InAs/GaAs Qdot laser under study is formed in the dots-in-a-well structure grown by solid source molecular beam epitaxy on a GaAs(100) substrate. The active region consists of six 9.1 nm thick DWELL layers with a dot area density of $\sim 1.3 \times 10^{11}$ cm^{-2}. The laser incorporates a chromium grating with a pitch of 200 nm to form a complex coupled distributed feedback structure. The cavity has a length of 300 μm and a ridge width of 3.5 μm. High-reflection facets of 80% at the front and 95% at the back are coated to enable a high-Q cavity [34,35]. Figure 1 shows the experimental setup for the investigation of P1 dynamics using the injection locking technique. A single-mode tunable laser is used as the master laser and the injected light is coupled into the Qdot laser through an optical circulator. The polarization of the injected light is carefully aligned with the Qdot laser by adjusting a polarization controller. The best alignment is indicated by a maximum redshift of the slave laser wavelength. Once aligned, the polarization is maintained during the measurements. The optical spectrum of the output light (10%) is collected by a high-resolution (10 pm) optical spectrum analyzer (OSA), while the electrical signal is analyzed by an electrical spectrum analyzer (ESA, 5 MHz resolution) via a photodiode (PD) with a bandwidth of 12 GHz. The temperature of the Qdot laser is maintained at 298 K (room temperature) throughout the experiment, and the laser threshold is $I_{th} = 7$ mA. In the measurements, the laser is biased at $1.6 \times I_{th}$ (avoiding excessive thermal heating at higher bias current). The coupled power in the fiber pigtail is 0.17 mW at the lasing wavelength of 1309.27 nm. In the measurements, the injection ratio R_{inj} is defined as the ratio of the power from the master laser to that of the free-running slave laser, where the optical powers are measured at the fiber pigtail of the Qdot laser. Meanwhile,

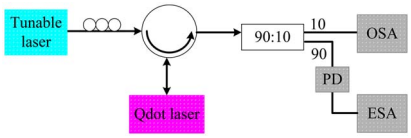

Fig. 1. Experimental setup of an optically injected Qdot laser for studying the P1 dynamics.

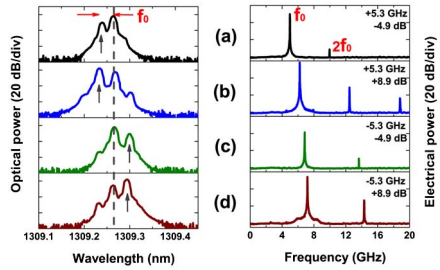

Fig. 2. Measured optical and electrical spectra at injection conditions (F_{inj}, R_{inj}) of (a) (5.3 GHz, −4.9 dB), (b) (5.3 GHz, 8.9 dB), (c) (−5.3 GHz, −4.9 dB), and (d) (−5.3 GHz, 8.9 dB). The dashed line is the central peak of the slave laser, and the gray arrows indicate the injected wave.

the detuning frequency F_{inj} is defined as the optical frequency difference between the master and the slave lasers.

Figure 2 presents the optical and electrical spectra of the Qdot laser at several injection conditions. The optical spectrum (left) is near-SSB, consisting of a stronger sideband regenerated from the master laser, the central peak by the slave laser, and a weaker sideband resulting from subsequent nonlinear wave-mixing effects [36–38]. Beating of the master and the slave optical components generates a fundamental microwave signal at f_0, as shown in the electrical spectra (right). In addition, second-order harmonics appear at $2 \times f_0$, which can induce nonlinear distortion of the microwave signals and thus should be suppressed in applications.

In the following mappings of the P1 dynamics, the injection ratio was increased by a step of around 0.50 dB and the frequency detuning by about 0.52 GHz. Figure 3(a) shows the microwave frequency map of the injection-locked Qdot laser. The white region (except chaos and P2) is stably locked, which is roughly bound by the Hopf bifurcation line at the positive detuning side and the saddle-node (SN) bifurcation line at the negative detuning side [1]. It is remarked that the Hopf line can also occur below the SN line in Qdot lasers as demonstrated in

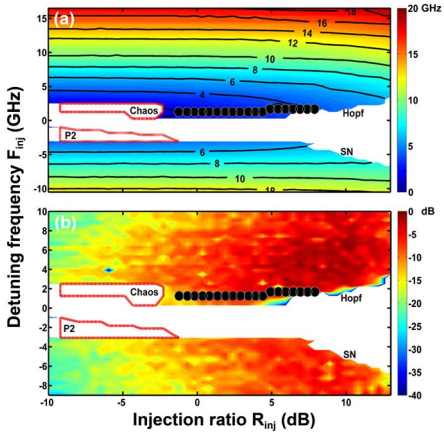

Fig. 3. Measured (a) microwave frequency f_0 and (b) microwave power of the optically injected Qdot laser. The microwave power is normalized to the maximum P1 power of −19.2 dBm at (F_{inj}, R_{inj}) = (6.3 GHz, 10.4 dB). The dots are oscillation points of low sensitivity to the frequency detuning. The P2 and chaos regions are bounded by the red lines.

Refs. [26,27]; however, the analysis of this Hopf bifurcation is out of the scope of this Letter. Immediately above the Hopf bifurcation, only a small region of chaos appears for $R_{inj} = -9.2 - 2.7$ dB with $F_{inj} = 1.2–2.5$ GHz. The chaotic oscillation is identified by a significantly broadened optical linewidth in combination with a broadband (several GHz) electrical spectrum [3,4]. On the other hand, a narrow region of period-two (P2) appears right below the SN bifurcation. These behaviors leave a wide space (colored regime) for the continuous photonic microwave generations. On one hand, the microwave signal is generated by undamping the relaxation oscillation (with a frequency of ~1.6 GHz) into P1 oscillations when the Qdot laser crosses the Hopf bifurcation line from the region of stable locking by increasing the detuning frequency. On the other hand, the microwave signal can also be generated by four-wave mixing (FWM) of the regenerated injection light and the emission light of the Qdot laser when it is operated under very weak injection strength or below the SN bifurcation line [28,29,39]. From the contour lines in the map, it is shown that the measured microwave frequency is continuously tuned up to 20 GHz by adjusting the detuning frequency. At large values of frequency detuning in the FWM regime, the microwave frequency is roughly equal to F_{inj} [7]. In contrast, the P1 frequency has little change with respect to the injection power. Especially for R_{inj} of less than 5.0 dB, the microwave frequency is nearly constant at a fixed detuning frequency, which is helpful to stabilize the microwave frequency against power fluctuations of the master laser and the Qdot laser. We remark that the P1 frequency evolution is qualitatively similar to that in a Qwell laser, as reported in [14]. However, the Qdot laser appears less sensitive to the injection power, which influences the P1 frequency through the α-factor [1]. This still requires quantitative experimental comparisons in future work. Interestingly, we retrieved some particular P1 oscillation points of low sensitivity to the frequency detuning denoted by the dots in Fig. 3(a), which will be discussed later in this Letter. Figure 3(b) illustrates the microwave power map of the injection-locked Qdot laser. The microwave power is normalized to the maximum value of −19.2 dBm, which is achieved at the injection condition $(R_{inj}, F_{inj}) = (10.4\ \text{dB}, 6.3\ \text{GHz})$. Generally, the microwave power increases with the injection strength except for operations close to the Hopf bifurcation, where it has a reduced sensitivity to the frequency detuning. Therefore, strong optical injection is preferable for enhancing the microwave power.

The SSB characteristics of the optical spectra can be quantified by the sideband rejection ratio, which is defined as the power ratio of the stronger sideband to the weaker sideband in the optical spectra (see Fig. 2) [7]. Figure 4(a) shows the sideband rejection ratio of the optical signal for injection ratios $R_{inj} = -1.0–13.0$ dB. For injection ratios below −1.0 dB, the second sideband peak power is too weak to extract and thus is not shown in the figure. From the contour lines, we can see the sideband rejection ratio increases with both the injection ratio and the detuning frequency, which is in good agreement with the theoretical study of conventional semiconductor lasers in [7]. Apart from the oscillation points with $F_{inj} = 0 - 5.0$ GHz, most microwave oscillations have a sideband rejection ratio of more than 20 dB up to as large as 45 dB, which can be practically regarded as pure SSB signals [7,40]. This SSB nature of the optical signal is highly desirable for minimizing

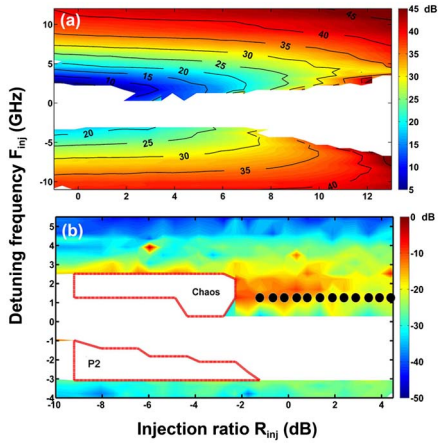

Fig. 4. (a) Measured optical sideband rejection ratio map of the injection-locked Qdot laser. (b) SHD map of the electrical signal. The symbols are of the same representations as in Fig. 3.

the fiber dispersion-induced power penalty of the microwave signals in the transmission. In the electrical spectra, the second-order harmonics can be characterized by the second-harmonic distortion (SHD), which is defined as the ratio of the second harmonic power at $2 \times f_0$, to the fundamental power at f_0 in the electrical spectra. The SHD of the optically injected Qdot laser is presented in Fig. 4(b). It is shown that the SHD of the microwave signal is usually less than −20 dB when the injection condition is away from the region of period-two and chaos oscillations. Increasing the detuning frequency larger than 5 GHz reduces the SHD value down to less than −35 dB. This experimental result is qualitatively in good agreement with the theoretical analysis of the P1 oscillation nonlinearity based on the consideration of the second-order harmonics in Ref. [41]. Suppression of the SHD to reduce this nonlinearity will be studied in future work.

Recently, microwave oscillation points insensitive to the detuning frequency have been pointed out to be of great importance [42,43]. These special operating points can stabilize the microwave frequency against the fluctuations in the detuning frequency. The points occur at the local minimum of the P1 frequency with respect to the detuning frequency as illustrated in Fig. 5(a). The local P1 frequency minimum is created by the combined effects of the redshift of the cavity resonance caused by the antiguidance effect governed by the α-factor and the Adler-type pulling effect governed by the phase dynamics of the laser [42,43]. Therefore, as shown in Fig. 3, the local minima (dots) always occur near the Hopf bifurcation line where the above two opposite effects balance out. Figure 5(b) shows that the microwave frequency of the detuning frequency insensitive points increases almost linearly with the injection ratio from 1.8 GHz at $R_{inj} = -2.8$ dB to 4.0 GHz at $R_{inj} = 6.4$ dB. Meanwhile, the microwave power is enhanced from −13.3 dB up to −3.0 dB. On the other hand, as presented in Fig. 5(c), the electrical SHD decreases to −25.6 dB, while the optical sideband rejection ratio increases to 24.7 dB at $R_{inj} = 6.4$ dB.

In conclusion, this work performs an experimental investigation of the P1 dynamics of an InAs/GaAs Qdot laser subject to optical injection. Owing to the small region of complex dynamics like high-order oscillations and chaos, the study unveils the potential of Qdot lasers for the realization of widely tunable

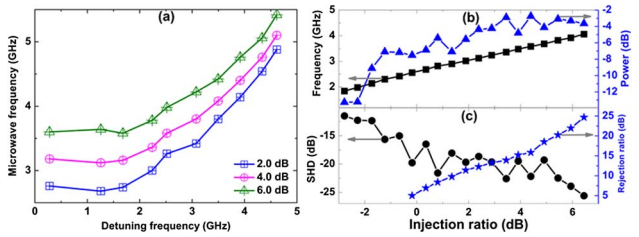

Fig. 5. (a) Illustration of the local minimum P1 frequency as a function of the detuning frequency at $R_{inj} = 2.0$, 4.0, and 6.0 dB. (b) Microwave frequency (square) and microwave power (triangle), (c) SHD (dot) and sideband rejection ratio (star) of the detuning frequency insensitive P1 oscillation points indicated in Fig. 3.

photonic microwave oscillators. To this end, it is demonstrated that strong injection strength does enhance the microwave power of the electrical signal and improve the SSB property of the optical signal, providing that the operation stays away from the Hopf bifurcation. Further improvements can be expected with Qdot lasers of a larger relaxation oscillation frequency, which can increase the tuning range [44,45]. On the other hand, large frequency detuning increases the microwave frequency, reduces the electrical SHD, and improves the optical SSB performance as well. Particularly, P1 oscillations of low sensitivity to the detuning frequency are found to occur near the Hopf bifurcation line of the optically injected Qdot laser. Future work will study the phase noise properties of the Qdot laser's P1 oscillation, as well as employing optical feedback techniques to reduce the microwave linewidth.

Funding. European Office of Aerospace Research and Development (FA9550-15-1-0104); National Natural Science Foundation of China (NSFC) (61308002); Research Grant Council of Hong Kong, China (CityU 11201014).

Acknowledgment. We thank E. Decerle from Yenista Optics in Lannion, France, for providing the tunable external cavity laser.

REFERENCES

1. S. Wieczorek, B. Krauskopf, T. Simpson, and D. Lenstra, Phys. Rep. **416**, 1 (2005).
2. A. Argyris, D. Syvridis, L. Larger, V. A. Lodi, P. Colet, I. Fischer, J. G. Ojalvo, C. R. Mirasso, L. Pesquera, and K. A. Shore, Nat. Photonics **438**, 343 (2005).
3. A. Uchida, K. Amano, M. Inoue, K. Hirano, S. Naito, H. Someya, I. OoWada, T. Kurashige, M. Shiki, S. Yoshimori, K. Yoshimura, and P. Davis, Nat. Photonics **2**, 728 (2008).
4. M. Sciamanna and K. A. Shore, Nat. Photonics **9**, 151 (2015).
5. X. Z. Li, S. S. Li, J. P. Zhuang, and S. C. Chan, Opt. Lett. **40**, 3970 (2015).
6. X. Q. Qi and J. M. Liu, IEEE J. Sel. Top. Quantum Electron. **17**, 1198 (2011).
7. S. C. Chan, S. K. Hwang, and J. M. Liu, Opt. Express **15**, 14921 (2007).
8. C. C. Cui, X. L. Fu, and S. C. Chan, Opt. Lett. **34**, 3821 (2009).
9. S. C. Chan, IEEE J. Quantum Electron. **46**, 421 (2010).
10. C. C. Cui and S. C. Chan, IEEE J. Quantum Electron. **48**, 490 (2012).
11. Y. H. Hung, C. H. Chu, and S. K. Hwang, Opt. Lett. **38**, 1482 (2013).
12. J. P. Zhuang and S. C. Chan, Opt. Lett. **38**, 344 (2013).
13. J. P. Zhuang and S. C. Chan, Opt. Express **23**, 2777 (2015).
14. S. K. Hwang, J. M. Liu, and J. K. White, IEEE J. Sel. Top. Quantum Electron. **10**, 974 (2004).
15. Y. S. Juan and F. Y. Lin, IEEE Photon. J. **3**, 644 (2011).
16. T. B. Simpson, J. M. Liu, M. AlMulla, N. G. Usechak, and V. Kovanis, IEEE J. Sel. Top. Quantum Electron. **19**, 1500807 (2013).
17. L. Fan, Z. M. Wu, T. Deng, J. G. Wu, X. Tang, J. J. Chen, S. Mao, and G. Q. Xia, J. Lightwave Technol. **32**, 4058 (2014).
18. P. Pérez, A. Quirce, A. Valle, A. Consoli, I. Noriega, L. Pesquera, and I. Esquivias, IEEE Photon. J. **7**, 5500614 (2015).
19. G. T. Liu, A. Stintz, H. Li, K. J. Malloy, and L. F. Lester, Electron. Lett. **35**, 1163 (1999).
20. D. G. Deppe, K. Shavritranuruk, G. Ozgur, H. Chen, and S. Freisem, Electron. Lett. **45**, 54 (2009).
21. S. S. Mikhrin, A. R. Kovsh, I. L. Krestnikov, A. V. Kozhukhov, D. A. Livshits, N. N. Ledentsov, Y. M. Shernyakov, I. I. Novikov, M. V. Maximov, V. M. Ustinov, and Z. I. Alferov, Semicond. Sci. Technol. **20**, 340 (2005).
22. D. Bimberg, M. Grundmann, and N. N. Ledentsov, *Quantum Dot Heterostructures* (Wiley, 1999).
23. A. E. Zhukov, M. V. Maximov, A. V. Savelyev, Y. M. Shernyakov, F. I. Zubov, V. V. Korenev, A. Martinez, A. Ramdane, J.-G. Provost, and D. A. Livshits, J. Appl. Phys. **113**, 233103 (2013).
24. D. Goulding, S. P. Hegarty, O. Rasskazov, S. Melnik, M. Hartnett, G. Greene, J. G. McInerney, D. Rachinskii, and G. Huyet, Phys. Rev. Lett. **98**, 153903 (2007).
25. B. Kelleher, C. Bonatto, G. Huyet, and S. P. Hegarty, Phys. Rev. E **83**, 026207 (2011).
26. T. Erneux, E. A. Viktorov, B. Kelleher, D. Goulding, S. P. Hegarty, and G. Huyet, Opt. Lett. **35**, 937 (2010).
27. B. Kelleher, D. Goulding, S. P. Hegarty, G. Huyet, E. A. Viktorov, and T. Erneux, *Quantum Dot Devices* (Springer, 2012).
28. J. Pausch, C. Otto, E. Tylaite, N. Majer, E. Schoell, and K. Lüdge, New J. Phys. **14**, 053018 (2012).
29. B. Lingnau, W. W. Chow, E. Schoell, and K. Lüdge, New J. Phys. **15**, 093031 (2013).
30. M. C. Pochet, N. A. Naderi, V. Kovanis, and L. F. Lester, IEEE J. Quantum Electron. **47**, 827 (2011).
31. M. C. Pochet, N. A. Naderi, Y. Li, V. Kovanis, and L. F. Lester, IEEE Photon. Technol. Lett. **22**, 763 (2010).
32. A. Hurtado, J. Mee, M. Nami, I. D. Henning, M. J. Adams, and L. F. Lester, Opt. Express **21**, 10772 (2013).
33. C. Y. Chen, C. H. Cheng, and F. Y. Lin, *The European Conference on Lasers and Electro-Optics* (2015).
34. H. Su, L. Zhang, A. L. Gray, R. Wang, T. C. Newell, K. J. Malloy, and L. F. Lester, IEEE Photon. Technol. Lett. **15**, 1504 (2003).
35. H. Su and L. F. Lester, J. Phys. D **38**, 2112 (2005).
36. A. Murakami, K. Kawashima, and K. Atsuki, IEEE J. Quantum Electron. **39**, 1196 (2003).
37. H. K. Sung, E. K. Lau, and M. C. Wu, IEEE Photon. Technol. Lett. **19**, 1005 (2007).
38. S. K. Hwang and D. H. Liang, Appl. Phys. Lett. **89**, 061120 (2006).
39. S. Wieczorek, T. B. Simpson, B. Krauskopf, and D. Lenstra, Phys. Rev. E **65**, 045207(R) (2002).
40. C. Lim, D. Novak, A. Nirmalathas, and G. H. Smith, IEEE Trans. Microwave Theory Tech. **49**, 288 (2001).
41. C. J. Lin, M. AlMulla, and J. M. Liu, IEEE J. Quantum Electron. **50**, 815 (2014).
42. T. B. Simpson, J. M. Liu, M. AlMulla, N. G. Usechak, and V. Kovanis, Phys. Rev. Lett. **112**, 023901 (2014).
43. M. AlMulla and J. M. Liu, IEEE J. Sel. Top. Quantum Electron. **21**, 601 (2015).
44. M. T. Crowley, N. A. Naderi, H. Su, F. Grillot, and L. F. Lester, *Advances in Semiconductor Lasers, Semiconductors and Semimetals* (Academic, 2012), Vol. **86**.
45. T. Erneux and P. Glorieux, *Lasers Dynamics* (Cambridge University, 2010).